

## Phase Diagram Determination to Elucidate the Crystal Growth of the Photoreaction Center from *Rhodobacter sphaeroides*

BY TAKAYUKI ODAHARA, MITSUO ATAKA AND TATSUO KATSURA

Department of Biomolecular Engineering, National Institute of Bioscience and Human Technology, 1-1 Higashi, Tsukuba, Ibaraki 305, Japan

(Received 5 January 1994; accepted 10 March 1994)

### Abstract

Solubility curves (a phase diagram) of an amorphous precipitate and the orthorhombic crystals of a membrane protein, the photoreaction center from *Rhodobacter sphaeroides*, were determined. With the phase diagram, the process of crystal growth of the membrane protein was elucidated within a general physicochemical framework, and justification was provided of hitherto empirically selected crystallization conditions.

### Introduction

Phase diagrams form the basis for the design of crystal growth conditions. However, in most of the reported protein crystallization experiments, changes in the protein concentration after the crystals have started growing have not been adequately described. It is only recently that the phase diagrams of protein crystals have started to be determined systematically (Ataka & Tanaka, 1986; Weber, 1991; Riès-Kautt & Ducruix, 1992; Ataka, 1993). Reports of the crystallization of the photoreaction center (PRC) of *Rhodospseudomonas viridis* (Michel, 1982; Deisenhofer, Epp, Miki, Huber & Michel, 1984, 1985; Deisenhofer & Michel, 1989), of *Rhodobacter sphaeroides* R-26 (Allen & Feher, 1984; Chang, Schiffer, Tiede, Smith & Norris, 1985; Chang *et al.*, 1986; Allen, Feher, Yeates, Komiya & Rees, 1987*a,b*) and the wild-type strain (Frank, Taremi & Knox, 1987; Ducruix & Reiss-Husson, 1987; Yeates *et al.*, 1988) suggest that even the crystallization of membrane proteins, notoriously difficult to handle, is now within our reach. We present here a phase diagram of the PRC from wild-type *R. sphaeroides*. Its successful establishment required the precise determination of each crystallization parameter and careful sample preparation. The results enable the growth of these crystals to be understood within a general physicochemical framework, provide a justification for hitherto empirically selected crystallization conditions, and offer rational guidelines for their improvement.

### Materials and methods

PRCs of wild-type *R. sphaeroides* were purified from pressure-disrupted cells by use of an additional step, molecular-sieve chromatography (CL-6B), to the method described by Frank *et al.* (1987), using lauryl dimethylamine oxide (LDAO) as a detergent. The detergent (*n*-octyl- $\beta$ -D-glucoside) used in the final protein solubilization and the precipitating agent

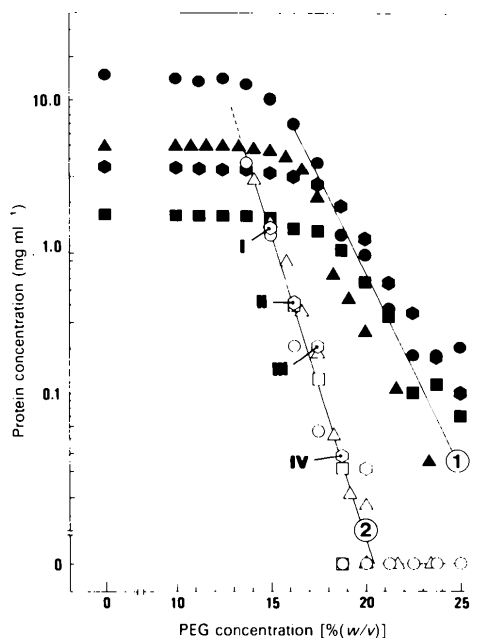


Fig. 1. Concentrations of PRCs from *R. sphaeroides* represented as a function of PEG concentration in a semi-logarithmic way. Filled symbols are the protein concentrations remaining in the supernatant immediately after removing the amorphous precipitate by centrifugation. Initial concentrations of PRC before removing the amorphous precipitate by centrifugation,  $C_0$ , were 14.5 (●), 4.7 (▲), 3.3 (◆) and 1.6 mg ml<sup>-1</sup> (■). The corresponding open symbols are the protein concentrations remaining in the supernatant, which equilibrated with the crystal phase, measured more than one month after crystal appearance. The solubility decreases steeply with PEG concentration; this is the basis for the use of PEG as a crystallizing agent. The diagram also indicates that PEG and protein concentrations are the principal parameters for crystallization. Points I, II, III and IV correspond to the crystals shown in Fig. 3.

[polyethylene glycol 4000 (PEG)] for the crystal growth were the same as those used in previously reported experiments (Allen & Feher, 1984; Chang *et al.*, 1985; Ducruix & Reiss-Husson, 1987; Frank *et al.*, 1987). The buffer used contained 10 mM Tris-HCl (pH 8.0), 1 mM EDTA, 0.05% (w/v)  $\text{NaN}_3$ , 0.8% (w/v) *n*-octyl- $\beta$ -D-glucoside, 1.0% (w/v) 1,2,3-heptanetriol and 200 mM NaCl. The crystallization solution was prepared by mixing PEG-containing buffer with the protein solution (final volume 0.2 ml) in a small test tube with a sealed cap. Initial protein concentrations ( $C_0$ ) before removing amorphous precipitate formed by the addition of PEG, were 14.5, 4.7, 3.3 or 1.6  $\text{mg ml}^{-1}$ . Crystallization was carried out in the dark at 298 K. The solubility of the protein at each PEG concentration was determined by measuring the absorbance of the supernatant obtained by centrifugation (6000g, 3 min). The relationship that one unit at 800 nm corresponds to 0.33  $\text{mg ml}^{-1}$  of the protein (Allen & Feher, 1984) was used.

### Results and discussion

We first established that the orthorhombic crystals grew in batches, in which the change of protein concentration with time could be measured under strictly fixed conditions. The hanging-drop vapor-diffusion method, commonly employed to date

(Michel, 1982; Allen & Feher, 1984; Chang *et al.*, 1985; Ducruix & Reiss-Husson, 1987; Frank *et al.*, 1987), is not suitable for the determination of phase diagrams, because the solution volume is too small and all the component concentrations vary with time.

The PEG concentration dependencies of the amorphous precipitate and crystal solubility are shown in Fig. 1. Upon the addition of a sufficient amount of PEG, an amorphous precipitate formed instantaneously. After immediately removing the precipitate by centrifugation, the protein concentration in the supernatant was determined (Fig. 1, filled symbols). It was necessary to use a PEG solution; the use of solid PEG gave less reproducible results. The amount of protein removed as precipitate increased steeply when the PEG concentration exceeded about 15% (w/v). Interestingly, the remaining protein concentration did not strongly depend on initial protein concentrations ( $C_0$ ); the precipitation on the addition of PEG appears to be almost over in a few minutes. All of the solutions thus cleared of the initial precipitate showed no evidence of additional precipitation two months later. We can thus define a boundary (curve ① in Figs. 1 and 2) representing the solution concentration that is in equilibrium with the amorphous precipitate. Since precipitate formation obscures the right-hand side of the curve, the region that we can use for crystallization is limited to that on the left-hand side.

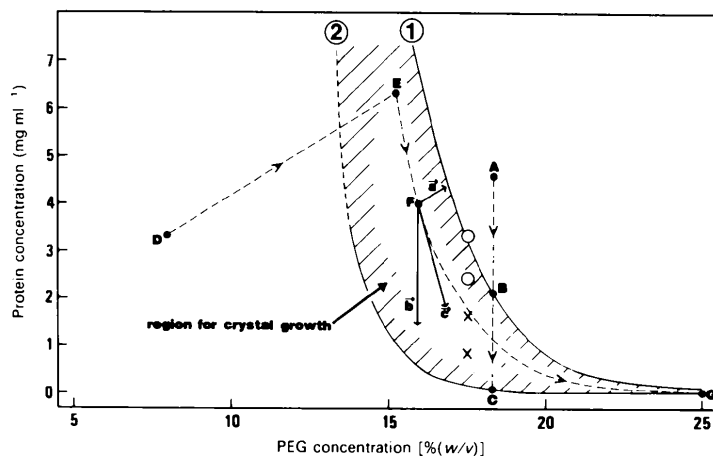


Fig. 2. Phase diagram representing crystal growth of PRCs from *R. sphaeroides*; curve ①, taken from Fig. 1, represents the equilibrium concentration with amorphous precipitate at room temperature and curve ②, also taken from Fig. 1, is the solubility of the crystals at 298 K. For example, in a batch with a  $C_0$  of 4.7  $\text{mg ml}^{-1}$  at 18.3% (w/v) of PEG, the concentration of the protein in the supernatant immediately decreased from A to B on addition of PEG and gradually decreased to the equilibrium concentration (C) as the crystal grew. On the other hand, by the vapor-diffusion method, the concentrations of protein and PEG first increase and enter into the supersaturated region along the line DE with evaporation of solvent water from the solution. When the solution reaches a state represented by point E, crystals start to form and then crystal growth is forced along the line EG which is determined both by the evaporation of solvent ( $\vec{a}$ ) and the driving force originating from the degree of supersaturation ( $\vec{b}$ ). The starting condition (point D) must be carefully chosen, as was indeed the case with Allen & Feher (1984), otherwise the solution condition may continue to change in the direction of the line DE, and amorphous precipitate will rapidly form, thus interfering with the growth of crystals. At a fixed PEG concentration of 17.5% (w/v), crystals grew within a week from the concentrations represented by open circles (○) but did not grow from those represented by crosses (×).

For  $C_0$  values of 14.5, 4.7, 3.3 and  $1.6 \text{ mg ml}^{-1}$ , crystallization was initiated when the PEG concentration exceeded 13.8, 14.2, 15.0 and 16.3% (w/v), respectively; the changes in the protein concentration in the supernatant due to crystal growth ended approximately two weeks after crystal appearance.

The supernatant concentration was determined again after more than one month, a period sufficient for the solution and crystals to reach an equilibrium. The results are included in Fig. 1 as open symbols. Again, the remaining protein concentration was determined almost solely by the PEG concentration. This led to the solubility curve for the crystals, curve ② in Figs. 1 and 2. We suggest that the reason for the smaller scatter of data points for the crystal than for the amorphous precipitate is the precise temperature control over a long period. The protein can

crystallize only on the right-hand side of the curve. Note the large difference between the two curves; it corresponds to the number of molecules available for crystallization ( $B \rightarrow C$  in Fig. 2).

This phase diagram is rather similar to the diagrams of other soluble proteins like, for instance, lysozyme (Ataka & Tanaka, 1986; Ducruix & Giegé, 1992; Riès-Kautt & Ducruix, 1992), confirming that a membrane protein can be treated in the same way as soluble proteins in crystallization. On the other hand, the crystallization characteristics of this protein are different from those of bovine heart cytochrome *c* oxidase, which crystallized in the low ionic strength region (Ataka, Shinzawa-Itoh & Yoshikawa, 1992).

The phase diagram provides a deeper insight into the path of crystal growth by vapor diffusion (Allen



Fig. 3. Photographs showing the effect of PEG concentration on the crystal size of PRCs from *R. sphaeroides*.  $C_0$  was  $3.3 \text{ mg ml}^{-1}$ , PEG concentrations were: 15.0 (I), 16.3 (II), 17.5 (III) and 18.8% (w/v) (IV) as shown in Fig. 1.

& Feher, 1984; Chang *et al.*, 1985; Ducruix & Reiss-Husson, 1987; Frank *et al.*, 1987), shown in Fig. 2. Point *D* represents the initial combination of PRC and PEG concentrations adopted by Allen & Feher (1984). The protein and PEG concentrations change along the line *DE*, passing through the origin, as water evaporates from the drop. When the solution conditions are sufficiently within the supersaturated region (for example, at the point *E*), crystal growth occurs. At this stage, the conversion of protein molecules into a crystalline phase and the evaporation of water progress simultaneously, so the solution conditions are expected to change along a curve such as *EG*. Here, the path ( $\vec{c}$ ) should be determined both by evaporation of solvent ( $\vec{a}$ ) and the driving force ( $\vec{b}$ ) as shown at the point *F* in Fig. 2. The point *G* is the solubility value we have determined for the PEG concentration in the reservoir solution used by Allen & Feher (1984).

Fig. 3 compares the crystal sizes obtained after one month when  $C_0$  was  $3.3 \text{ mg ml}^{-1}$ . Larger crystals were obtained from solutions with lower PEG concentrations; a similar tendency was pointed out by Michel for the crystallization of PRCs from *R. viridis* (Michel, 1982). This tendency is confirmed by our phase diagram, since the ratio of  $C_0$  to the solubility (degree of supersaturation) is the thermodynamical driving force both for nucleation and for crystal growth (Mikol & Giegé, 1992).

With the phase diagram at hand, we can further modify the crystallization conditions. For example, an adjustment of the starting protein concentration,  $C_0$ , helps determine the driving force for crystallization. This will be reflected in the number and the size of the crystals and/or the delay time for their appearance. We examined crystal growth as a function of protein concentration (3.5, 2.5, 1.7 and  $0.8 \text{ mg ml}^{-1}$  of PRC) at a fixed PEG concentration of 17.5% (w/v). Crystals were obtained within one week only when the starting concentrations were 3.5 and  $2.5 \text{ mg ml}^{-1}$  (open circles in Fig. 2). This indicates that a certain critical supersaturation is needed for crystallization, even within the supersaturation region.

It has been shown that a phase diagram, which describes the physicochemical basis of crystal

growth, can be determined for a membrane protein. Successful understanding of the crystallization of a membrane protein with the use of a phase diagram should encourage others to adopt a similar approach when the crystal growth of a new membrane protein is being attempted.

We are grateful to S. Vigmond of the National Institute of Bioscience and Human Technology for his careful reading of the manuscript.

#### References

- ALLEN, J. P. & FEHER, G. (1984). *Proc. Natl Acad. Sci. USA*, **81**, 4795–4799.
- ALLEN, J. P., FEHER, G., YEATES, T. O., KOMIYA, H. & REES, D. C. (1987a). *Proc. Natl Acad. Sci. USA*, **84**, 5730–5734.
- ALLEN, J. P., FEHER, G., YEATES, T. O., KOMIYA, H. & REES, D. C. (1987b). *Proc. Natl Acad. Sci. USA*, **84**, 6162–6166.
- ATAKA, M. (1993). *Phase Transit.* **45**, 205–219.
- ATAKA, M., SHINZAWA-ITOH, K. & YOSHIKAWA, S. (1992). *J. Cryst. Growth*, **122**, 60–65.
- ATAKA, M. & TANAKA, S. (1986). *Biopolymers*, **25**, 337–350.
- CHANG, C.-H., SCHIFFER, M., TIEDE, D., SMITH, U. & NORRIS, J. (1985). *J. Mol. Biol.* **186**, 201–203.
- CHANG, C.-H., TIEDE, D., TANG, J., SMITH, U., NORRIS, J. & SCHIFFER, M. (1986). *FEBS Lett.* **205**, 82–86.
- DEISENHOFER, J., EPP, O., MIKI, K., HUBER, R. & MICHEL, H. (1984). *J. Mol. Biol.* **180**, 385–398.
- DEISENHOFER, J., EPP, O., MIKI, K., HUBER, R. & MICHEL, H. (1985). *Nature (London)*, **318**, 618–624.
- DEISENHOFER, J. & MICHEL, H. (1989). *Science*, **245**, 1463–1473.
- DUCRUIX, A. & GIEGÉ, R. (1992). *Crystallization of Nucleic Acids and Proteins*, edited by A. DUCRUIX & R. GIEGÉ, pp. 73–98. Oxford: IRL Press.
- DUCRUIX, A. & REISS-HUSSON, F. (1987). *J. Mol. Biol.* **193**, 419–421.
- FRANK, H. A., TAREMI, S. S. & KNOX, J. R. (1987). *J. Mol. Biol.* **198**, 139–141.
- MICHEL, H. (1982). *J. Mol. Biol.* **158**, 567–572.
- MIKOL, V. & GIEGÉ, R. (1992). *Crystallization of Nucleic Acids and Proteins*, edited by A. DUCRUIX & R. GIEGÉ, pp. 219–239. Oxford: IRL Press.
- RIÈS-KAUTT, M. & DUCRUIX, A. (1992). *Crystallization of Nucleic Acids and Proteins*, edited by A. DUCRUIX & R. GIEGÉ, pp. 195–218. Oxford: IRL Press.
- WEBER, P. C. (1991). *Adv. Protein Chem.* **41**, 1–36.
- YEATES, T. O., KOMIYA, H., CHIRINO, A., REES, D. C., ALLEN, J. P. & FEHER, G. (1988). *Proc. Natl Acad. Sci. USA*, **85**, 7993–7997.